Multi-UAV Safe Collaborative Transportation Based on Adaptive Control Barrier Function

Zhijun Wang, Tengfei Hu, and Lijun Long, *Member, IEEE*

***Abstract*—This article focuses on the problem of adaptive safe stabilization for a class of nonlinear control affine systems with parameter uncertainties. Two novel definitions of adaptive control Lyapunov function (ACLF) and adaptive control barrier function (ACBF) are first introduced, which use multiple identification models combined with a logic switching mechanism for parameter adaptation. The switching mechanism can improve the transient performance of nonlinear systems. Also, a multiunmanned aerial vehicle (multi-UAV) safe collaborative transportation framework based on ACLF and ACBF is provided in the presence of parametric uncertainties, in which a nominal controller is derived by using the proposed ACLF with a quadratic programming (QP) algorithm, and the nominal controller is further modified by the ACBF-QP algorithm for safety filter to achieve adaptive safe stabilization. Finally, simulation results for safe collaborative transportation of dual unmanned aerial vehicles in three-dimensional space are presented to demonstrate the effectiveness of the proposed design approach.**

***Index Terms*—Adaptive control barrier function (ACBF), adaptive control Lyapunov function (ACLF), adaptive safe stabilization, quadratic programming (QP), safety filter.**

I. Introduction

IN RECENT decades, unmanned aerial vehicles (UAVs) have been widely used in a variety of fields, including military reconnaissance, emergency rescue, light shows, and so on [1], [2]. As the difficulty of mission requirements increases, it is often challenging for mono-UAV to meet mission requirements, and then it becomes crucial for multiunmanned aerial vehicle (multi-UAV) to work together [3], [4]. In particular, multi-UAV collaborative transportation requires not only transporting the payload to the desired position but also avoiding the possibility of collision with obstacles [5]. In fact, the essence of obstacle avoidance is a safety-critical control problem. The notion of safety-critical control is used to illustrate that the primary control objective of a system is to achieve safety. Safety-critical control algorithms for obstacle avoidance have been widely studied [6], [7], [8]. For instance, global path planning can plan an optimal path in an environment with obstacles [6], in which this algorithm requires accurate information about the environment to be known in advance. When the environment changes, such as the presence of unknown obstacles, the algorithm is powerless. In addition, local path planning is also an important obstacle avoidance algorithm. This algorithm is to detect the working environment by sensors when the environmental information is completely unknown or partially knowable, so that the local path can be planned by real-time data, but the planning result may not be optimal because of the lack of global environmental information [7].

Recently, a new safety-critical control algorithm, i.e., control barrier function (CBF) is proposed in [8], and a safety controller is obtained by solving CBF-quadratic programming (QP). Compared with other safety control algorithms, the CBF has the following advantages. First, this algorithm can achieve optimal safety control by solving a QP problem. Second, safety (hard constraint) and stability (soft constraint) can be achieved simultaneously. Third, it is easier to achieve safety control for nonlinear systems with parameter uncertainties. Also, the algorithm requires less computational capability to solve the controller compared to path planning. More recently, this algorithm has been applied in many fields, such as bipedal robots, adaptive cruise systems, and UAVs [8], [9], [10]. Also, safety-critical control for switched systems and event-triggered control based on the CBF have been studied [11], [12], [13]. Meanwhile, many algorithms for stability control have been proposed, such as proportional integral derivative (PID), control Lyapunov function (CLF), model predictive control (MPC), and linear quadratic regulator (LQR) [14], [15], [16], [17], in which CLF is an important tool of classical control theory, and it has pivotal importance in stability analysis [15]. In order to achieve safe stabilization, safety control algorithms always need to be combined with stability algorithms. For instance, a common algorithm currently used to achieve safe stabilization is to unify CLF and CBF in the QP framework [18]. However, less attention about how to achieve safe stabilization has been paid to nonlinear systems with parameter uncertainties until now.

This article focuses on nonlinear control affine systems with parameter uncertainties. For such system, the main

Manuscript received 27 November 2022; revised 11 June 2023; accepted 1 July 2023. This work was supported in part by the National Natural Science Foundation of China under Grant 62173075 and Grant 61773100; in part by the 111 Project under Grant B16009; in part by the Liaoning Revitalization Talents Program under Grant XLYC1907043; and in part by the Fundamental Research Funds for the Central Universities under Grant N2004015. This article was recommended by Associate Editor Z. Peng. *(Corresponding author: Lijun Long.)*

Zhijun Wang and Tengfei Hu are with the College of Information Science and Engineering, Northeastern University, Shenyang 110819, China (e-mail: zhijunwang2022@126.com; 1900797@stu.neu.edu.cn).

Lijun Long is with the College of Information Science and Engineering and the State Key Laboratory of Synthetical Automation for Process Industries, Northeastern University, Shenyang 110819, China (e-mail: longlijun@ise.neu.edu.cn).

Color versions of one or more figures in this article are available at https://doi.org/10.1109/TSMC.2023.3292810.

Digital Object Identifier 10.1109/TSMC.2023.3292810

problem is how to deal with parameter uncertainties. At present, adaptive control is a popular approach to address this problem [19]. Various adaptive control algorithms have been proposed in [19], [20], and [21]. Also, [22] extends adaptive stabilization to adaptive safety, yielding a new definition of adaptive CBF (ACBF) that allows for safety control of nonlinear systems with parametric uncertainties. Thereafter, robust ACBF (RaCBF) combined with data-driven-based set membership identification method has been introduced in [23]. A unification of CLF or CBF with techniques from concurrent learning (CL) adaptive control has been proposed in [24] and [25]. Bayesian learning methods using Gaussian process regression (GPR) have been also proposed to learn state-dependent uncertainties [26], [27]. All of the aforementioned methods are effective design tools in ensuring the safety or stability of nonlinear systems in the presence of uncertainties. However, some of the mentioned methods do not achieve safety and stability at the same time. Also, a well-known problem for the mentioned methods is that the transient performance is usually quite bad, especially when there exist large initial estimation errors [31]. Therefore, it is important to establish a method to ensure adaptive safe stabilization and improve the transient performance of nonlinear control affine systems with parameter uncertainties.

Motivated by the use of multiple identification models combined with a proper logic switching mechanism for nonlinear control affine systems in [31] and a control framework is established for safe collaborative transportation of multi-UAV in [28]. Compared with the existing results on safe stabilization of uncertain nonlinear systems, the main contributions of this article are summarized as follows.

1) Two novel definitions of adaptive CLF (ACLF) and ACBF based on multiple identification models are presented for a class of nonlinear control affine systems with parametric uncertainties. Also, multiple identification models are used for parametric adaptation. To the best of our knowledge, no results on adaptive safe stabilization are available through multiple identification models until now.
2) Compared to the existing results in [22], [23], [24], [25], [26], and [27], in order to address the problem of poor transient performance when there exist large initial parameter estimation errors, a logic switching mechanism is used to improve the transient performance of nonlinear systems.
3) The classical CLF-CBF-QP method in [8] will be more difficult or even unsolvable when the number of constraints increases. Therefore, instead of choosing the CLF-CBF-QP structure, an ACLF-QP solving for a nominal controller is adopted, then, the nominal controller is further modified by ACBF-QP provided for safety filter to achieve adaptive safe stabilization in this article. In this way, we reduce the number of single QP constraints by splitting the ACLF-ACBF-QP into the ACLF-QP and the ACBF-QP, thus the solvability of the QP problem is increased.
4) Different from the existing result in [28], this article considers a multi-UAV safe collaborative transportation framework for the system model with parameter uncertainties.

The remainder of this article is organized as follows. Some basic preliminaries are presented in Section II. Section III illustrates multiple identification models, a logic switching scheme, and two new definitions of ACLF and ACBF. Section IV illustrates the framework for multi-UAV safe cooperative transportation. Simulation results of the proposed design approach are shown in Section V. Conclusions are drawn in Section VI.

Notations: The interval $[0, \infty)$ in the space of real numbers $\mathbb{R}$ is denoted by $\mathbb{R}^+$. $\mathbb{R}^n$ denotes the n-dimensional real Euclidean space. $|\cdot|$ denotes the absolute value. $\|\cdot\|$ denotes the Euclidean norm of vectors. $\|\cdot\|_F$ denotes the Frobenius norm of matrices. I_n denotes the n-dimensional identity matrix. $\langle x, y\rangle$ denotes the inner product between two vectors $x, y \in \mathbb{R}^n$. The superscript operator T denotes the vector transpose. ∂C and $\text{Int}(C)$ denotes the boundary and its interior of a set C, respectively. A function $\alpha : (-b, a) \to (-\infty, \infty)$ is said to be of extended class K for some $a, b > 0$ if it is continuous, strictly increasing and $\alpha(0) = 0$.

II. Preliminaries

Consider a nonlinear control affine system with parametric uncertainties

$$\dot{x} = f(x) + Y(x)\theta + g(x)u \tag{1}$$

where $x \in \mathbb{R}^n$ is the system state, $u \in U \subseteq \mathbb{R}^m$ (U denotes the input constraint set) is the control input, $\theta \in \mathbb{R}^q$ is an unknown constant parameter vector, $f(x) : \mathbb{R}^n \to \mathbb{R}^n$, $Y(x) : \mathbb{R}^n \to \mathbb{R}^{n\times q}$, and $g(x) : \mathbb{R}^n \to \mathbb{R}^{n\times m}$ are locally Lipschitz. It is assumed that for any initial condition $x_0 \in \mathbb{R}^n$, there exists a maximum interval of existence $\mathbf{I}(x_0) = [0, \tau_{\max})$, such that $x(t)$ is the unique solution to (1) on $\mathbf{I}(x_0)$; in the case when $f(x)$ is forward complete, $\tau_{\max} = \infty$.

Assumption 1 [30]: The unknown constant parameter vector θ belongs to a known compact set $S \subset \mathbb{R}^q$.

Remark 1: Assumption 1 implies that for any given estimated parameter $\hat{\theta} \in S$, there exists some maximum possible estimation error $\tilde{\vartheta} \in \mathbb{R}^q$ in the sense that $\|\theta - \hat{\theta}\| \leq \|\tilde{\vartheta}\|$ for all $\hat{\theta} \in S$. Given a compact set S, each component of $\tilde{\vartheta}$ can be computed as $\tilde{\vartheta}_i = \max_{\theta_i, \hat{\theta}_i \in S} |\theta_i - \hat{\theta}_i|$, $i = 1, \ldots, q$, where θ_i and $\hat{\theta}_i$ denote the ith component of θ and $\hat{\theta}$ [30].

A set C is defined as zero-superlevel set of a continuously differentiable function $h(x) : \mathbb{R}^n \to \mathbb{R}$

$$C = \left\{x \in \mathbb{R}^n : h(x) \geq 0\right\} \tag{2a}$$

$$\partial C = \left\{x \in \mathbb{R}^n : h(x) = 0\right\} \tag{2b}$$

$$\text{Int}(C) = \left\{x \in \mathbb{R}^n : h(x) > 0\right\}. \tag{2c}$$

We refer to C as the safe set.

Definition 1 (Forward Invariant and Safety [29]): The set C is forward invariant if for every $x_0 \in C$, $x(t) \in C$ for all $t \in \mathbf{I}(x_0)$. The system (1) is safe with respect to the set C if the set C is controlled invariant.

Our control objective is to solve the adaptive safe stabilization problem for the system (1) by designing a suitable logic switching mechanism.

III. Main Results

A. Multiple Identification Models

Consider N identification models $\{E_j\}_{j=1}^N$ with a same system structure. Also, those models have different initial estimated parameters $\hat{\theta}_1(0), \hat{\theta}_2(0), \ldots, \hat{\theta}_N(0)$, which are uniformly distributed in the compact set S. Then, we introduce the following filters in [19]:

$$\dot{\Omega}_0 = \left[A_0 - \mu Y(x)Y(x)^{\mathrm{T}}P\right](\Omega_0 - x) + f(x) + g(x)u,\ \Omega_0 \in \mathbb{R}^n \quad (3)$$

$$\dot{\Omega}^{\mathrm{T}} = \left[A_0 - \mu Y(x)Y(x)^{\mathrm{T}}P\right]\Omega^{\mathrm{T}} + Y(x),\ \Omega \in \mathbb{R}^{q\times n} \quad (4)$$

where μ is a positive constant and A_0 is a Hurwitz matrix, such that the Lyapunov equation $PA_0 + A_0^{\mathrm{T}}P = -I$ has a positive-definite solution P. In order to eliminate the disturbing effect of the initial estimation error, let us choose the initial filter states as $\Omega(0) = 0$ and $\Omega_0(0) = x_0$ [19].

Define

$$\omega_j = x - \Omega_0 - \Omega^{\mathrm{T}}\hat{\theta}_j,\ j = 1, \ldots, N \quad (5)$$

$$\tilde{\omega} = x - \Omega_0 - \Omega^{\mathrm{T}}\theta \quad (6)$$

$$\tilde{\theta}_j = \theta - \hat{\theta}_j,\ j = 1, \ldots, N. \quad (7)$$

By direct calculation, one has

$$\omega_j = \Omega^{\mathrm{T}}\tilde{\theta}_j + \tilde{\omega},\ j = 1, \ldots, N \quad (8)$$

$$\dot{\tilde{\omega}} = \dot{x} - \dot{\Omega}_0 - \dot{\Omega}^{\mathrm{T}}\theta = \left(A_0 - \mu Y(x)Y(x)^{\mathrm{T}}P\right)\tilde{\omega} \quad (9)$$

It is easy to see that $\tilde{\omega}$ decays exponentially, and (8) are called identification equations. Now, for the N identification models, design the following update laws:

$$\dot{\hat{\theta}}_j = \frac{\Omega\omega_j}{1 + \rho\|\Omega\|_F^2},\ \rho \geq 0,\ j = 1, \ldots, N \quad (10)$$

which share the same filter variables Ω and Ω_0.

Lemma 1: Consider the system (1) and suppose that the estimated parameters are updated by (10), Assumption 1 holds and initial estimates of parameters for different models $\hat{\theta}_1(0), \hat{\theta}_2(0), \ldots, \hat{\theta}_N(0)$ belong to the compact set S, then, the parameter estimation error $\tilde{\theta}_j = \theta - \hat{\theta}_j$ is bounded for all $t \geq 0$ as

$$\|\tilde{\theta}_j(t)\| \leq \varphi := \|\tilde{\vartheta}\|e^{-\int_0^t \frac{\lambda_{\min}(\tau)}{1+\rho\|\Omega\|_F^2}d\tau},\ j = 1, \ldots, N \quad (11)$$

where $\lambda_{\min}$ represents the minimum eigenvalue of $\Omega\Omega^{\mathrm{T}}$.

Proof: Since initial filter states are chosen as $\Omega(0) = 0$ and $\Omega_0(0) = x_0$, it is easy to obtain by (6) that $\tilde{\omega}(0) = 0$. Furthermore, by (9), one obtains $\tilde{\omega}(t) \equiv 0$. Then, (8) can be rewritten as

$$\omega_j = \Omega^{\mathrm{T}}\tilde{\theta}_j,\ j = 1, \ldots, N. \quad (12)$$

Let $V_j = \frac{1}{2}\tilde{\theta}_j^{\mathrm{T}}\tilde{\theta}_j$, one has

$$\begin{aligned}\dot{V}_j &= -\tilde{\theta}_j^{\mathrm{T}}\dot{\hat{\theta}}_j = -\tilde{\theta}_j^{\mathrm{T}}\frac{\Omega\omega_j}{1 + \rho\|\Omega\|_F^2} \\ &= -\frac{\tilde{\theta}_j^{\mathrm{T}}\Omega\Omega^{\mathrm{T}}\tilde{\theta}_j}{1 + \rho\|\Omega\|_F^2} \\ &\leq -\frac{2\lambda_{\min}V_j}{1 + \rho\|\Omega\|_F^2}. \end{aligned} \quad (13)$$

By integrating the above inequality, one further has

$$V_j(t) \leq V_j(0)e^{-\int_0^t \frac{2\lambda_{\min}(\tau)}{1+\rho\|\Omega\|_F^2}d\tau} \quad (14)$$

which implies that

$$\begin{aligned}\|\tilde{\theta}_j(t)\| &\leq \|\tilde{\theta}_j(0)\|e^{-\int_0^t \frac{\lambda_{\min}(\tau)}{1+\rho\|\Omega\|_F^2}d\tau} \\ &\leq \varphi := \|\tilde{\vartheta}\|e^{-\int_0^t \frac{\lambda_{\min}(\tau)}{1+\rho\|\Omega\|_F^2}d\tau} \end{aligned} \quad (15)$$

where $\tilde{\theta}_j(0) = \theta - \hat{\theta}_j(0),\ j = 1, \ldots, N.$ ■

B. Design of Switching Mechanism

This section will design a logic switching mechanism to improve transient performance. This mechanism determines online, where the identification model is selected by a performance criterion $\{J_j(t)\}_{j=1}^N$ based on the following identification errors $\omega_j, j = 1, \ldots, N$, in (8)

$$J_j(t) = \alpha\omega_j^2(t) + \beta\int_0^t \omega_j^2(\tau)d\tau,\ \alpha,\ \beta > 0,\ j = 1, \ldots, N. \quad (16)$$

Inspired by [31], design the following logic switching mechanism.

1) *Initialization:* Preselect two positive constants $T_{\min}$ and ξ. Also, we initialize the first identification model E_1 as the current model E_c, and E_c does not switch in the ensuring $T_{\min}$ time interval.
2) *Switching Mechanism:* At each time $t > 0$, if $\min_{j=1,\ldots,N} J_j(t) \leq J_c(t) - \xi$, where J_c represents the performance criterion of the current model E_c, then set $J_{j^*}(t) = \min_{j=1,\ldots,N} J_j(t)$. If in the successive ensuring $T_{\min}$ time interval, the inequality $J_{j^*}(t) \leq J_c(t) - \xi$ still holds, then, the current model E_c is reset with model E_{j^*}, and the estimate parameters are obtained from the j^*th model. Otherwise, the current model E_c remains unchanged and the process is then repeated. In order to facilitate the subsequent processing, the j^*th model denotes the selected model through the switching mechanism.

The block diagram of the logic switching mechanism is depicted as shown in Fig. 1.

Remark 2: By designing the suitable logic switching mechanism, the estimated parameters $\hat{\theta}$ close to the unknown parameters θ can be selected quickly, so that transient performance can be improved significantly.

C. Adaptive Control Lyapunov Function

Definition 2 (ACLF): A continuously differentiable function $V : \mathbb{R}^n \to \mathbb{R}$ is an ACLF for the system (1) if there exist positive constants c_1, c_2, c_3, such that for all $x \in \mathbb{R}^n$ and $\theta \in \mathbb{R}^q$

$$c_1\|x\|^2 \leq V(x)\ \leq c_2\|x\|^2 \quad (17)$$

$$\inf_{u\in U}\left[L_fV(x) + L_YV(x)\theta + L_gV(x)u + \|L_YV(x)\|\varphi\right] \leq -c_3V(x) \quad (18)$$

where φ is defined as in (11).

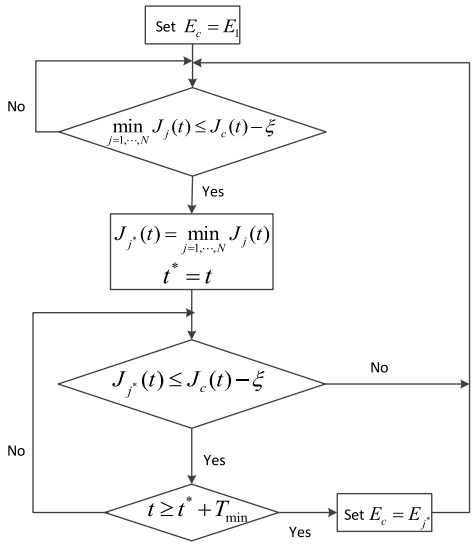

Fig. 1. Block diagram of the logic switching mechanism.

By means of Definition 2, the pointwise set of all stabilizing control values in the presence of parameter uncertainties is denoted by

$$K_{\text{ACLF}}(x,\theta) := \{u \in U | L_f V(x) + L_Y V(x)\theta + L_g V(x)u + \|L_Y V(x)\|\varphi \le -c_3 V(x)\}. \tag{19}$$

Theorem 1: Consider the system (1) and let a continuously differentiable function $V : \mathbb{R}^n \to \mathbb{R}$ is an *ACLF* as in Definition 2. If Assumption 1 holds and the estimated parameters are updated by (10), then any controller $u = \mathbf{k}(x, \hat{\theta}_{j^*})$ satisfying $\mathbf{k}(x, \hat{\theta}_{j^*}) \in K_{\text{ACLF}}(x, \hat{\theta}_{j^*})$ renders stable for the system (1).

Proof: In order to guarantee the stability of the system (1), it is sufficient to show that for each $x \in \mathbb{R}^n$, the input is selected, such as $\dot{V}(x) \le -c_3 V(x)$, where $\dot{V}(x) = L_f V(x) + L_Y V(x)\theta + L_g V(x)u$. Our aim is to show that any $u = \mathbf{k}(x, \hat{\theta}_{j^*}) \in K_{\text{ACLF}}(x, \hat{\theta}_{j^*})$ satisfies $L_f V(x) + L_Y V(x)\theta + L_g V(x)\mathbf{k} \le -c_3 V(x)$ for all $x \in \mathbb{R}^n$, and $\hat{\theta}_{j^*}$ is given by (10). To this end, observe that by Lemma 1 and the logic switching mechanism, under controller $u = \mathbf{k}(x, \hat{\theta}_{j^*}) \in K_{\text{ACLF}}(x, \hat{\theta}_{j^*})$

$$\begin{aligned}\dot{V}(x) &= L_f V(x) + L_Y V(x)\theta + L_g V(x)\mathbf{k}\\ &= L_f V(x) + L_Y V(x)\tilde{\theta}_{j^*} + L_Y V(x)\hat{\theta}_{j^*} + L_g V(x)\mathbf{k}\\ &\le L_f V(x) + L_Y V(x)\hat{\theta}_{j^*} + L_g V(x)\mathbf{k} + \|L_Y V(x)\|\|\tilde{\theta}_{j^*}\|\\ &\le L_f V(x) + L_Y V(x)\hat{\theta}_{j^*} + L_g V(x)\mathbf{k} + \|L_Y V(x)\|\varphi\\ &\le -c_3 V(x)\end{aligned} \tag{20}$$

for all $x \in \mathbb{R}^n$ and $\hat{\theta}_{j^*}$ is given by (10). In (20), the first inequality follows from the fact that $L_Y V(x)\tilde{\theta}_{j^*} \le \|L_Y V(x)\|\|\tilde{\theta}_{j^*}\|$, the second from the bound in (11), and the third from $u = \mathbf{k}(x, \hat{\theta}_{j^*}) \in K_{\text{ACLF}}(x, \hat{\theta}_{j^*})$. ■

D. Adaptive Control Barrier Function

Definition 3 (ACBF): Given a set $C \subset \mathbb{R}^n$ defined by (2a)–(2c) for a continuously differentiable function $h : \mathbb{R}^n \to \mathbb{R}$, the function h is called an ACBF defined on set C, if there exists an extended class K function α, such that for all $x \in C$ and $\theta \in \mathbb{R}^q$

$$\sup_{u \in U}\left[L_f h(x) + L_Y h(x)\theta + L_g h(x)u - \|L_Y h(x)\|\varphi\right] \ge -\alpha(h(x)) \tag{21}$$

where φ is defined as in (11).

According to Definition 3, the pointwise set of all safe control values in the presence of parameter uncertainties is denoted by

$$K_{\text{ACBF}}(x,\theta) := \{u \in U | L_f h(x) + L_Y h(x)\theta + L_g h(x)u - \|L_Y V(x)\|\varphi \ge -\alpha(h(x))\}. \tag{22}$$

Theorem 2: Consider the system (1), a set $C \subset \mathbb{R}^n$ defined by a continuously differentiable function $h : \mathbb{R}^n \to \mathbb{R}$ as in (2a)–(2c) and let h is an ACBF. If Assumption 1 holds and the estimated parameters are updated by (10), then any controller $u = \mathbf{k}(x, \hat{\theta}_{j^*})$ satisfying $\mathbf{k}(x, \hat{\theta}_{j^*}) \in K_{\text{ACBF}}(x, \hat{\theta}_{j^*})$ renders set C forward invariant for the system (1).

Proof: In order to guarantee forward invariant of safe set C, it is sufficient to show that for each $x \in C$, the input is selected such as $\dot{h}(x) \ge -\alpha(h(x))$. For the system (1), $\dot{h}(x) = L_f h(x) + L_Y h(x)\theta + L_g h(x)u$. Our aim is to show that any $u = \mathbf{k}(x, \hat{\theta}_{j^*}) \in K_{\text{ACBF}}(x, \hat{\theta}_{j^*})$ satisfies $L_f h(x) + L_Y h(x)\theta + L_g h(x)\mathbf{k} \ge -\alpha(h(x))$ for all $x \in C$, and $\hat{\theta}_{j^*}$ is given by (10). To this end, observe that by Lemma 1 and the logic switching mechanism, under controller $u = \mathbf{k}(x, \hat{\theta}_{j^*}) \in K_{\text{ACBF}}(x, \hat{\theta}_{j^*})$

$$\begin{aligned}\dot{h}(x) &= L_f h(x) + L_Y h(x)\theta + L_g h(x)\mathbf{k}\\ &= L_f h(x) + L_Y h(x)\tilde{\theta}_{j^*} + L_Y h(x)\hat{\theta}_{j^*} + L_g h(x)\mathbf{k}\\ &\ge L_f h(x) + L_Y h(x)\hat{\theta}_{j^*} + L_g h(x)\mathbf{k} - \|L_Y h(x)\|\|\tilde{\theta}_{j^*}\|\\ &\ge L_f h(x) + L_Y h(x)\hat{\theta}_{j^*} + L_g h(x)\mathbf{k} - \|L_Y h(x)\|\varphi\\ &\ge -\alpha(h(x))\end{aligned} \tag{23}$$

for all $x \in C$, and $\hat{\theta}_{j^*}$ is given by (10). In (23), the first inequality follows from the fact that $L_Y h(x)\tilde{\theta}_{j^*} \ge -\|L_Y h(x)\|\|\tilde{\theta}_{j^*}\|$, the second from the bound in (11), and the third from $u = \mathbf{k}(x, \hat{\theta}_{j^*}) \in K_{\text{ACBF}}(x, \hat{\theta}_{j^*})$. ■

IV. Multi-UAV Safe Collaborative Transportation

This section considers a multi-UAV safe collaborative transportation control framework as illustrated in Fig. 2. In Fig. 2, x_r, y, u_{ref}, and u denote the reference trajectory, the output, the nominal controller and the real control input, respectively. We carry out a three-part design for multi-UAV safe collaborative transportation control: 1) the nominal controller u_{ref} is designed by ACLF-QP; 2) the rigid body constraint is considered to ensure that the rigid payload avoids deformation; and 3) the obstacle avoidance is realized by a safety filter based on an ACBF-QP.

Assumption 2: The payload is a rigid body that is transported by dual UAVs. Moreover, the rigid body is connected to the UAVs by spherical joints.

Remark 3: Assumption 2 ensures that the flexibility can be improved and rigid body deformations can be ignored in practice by means of spherical joint connection. In addition,

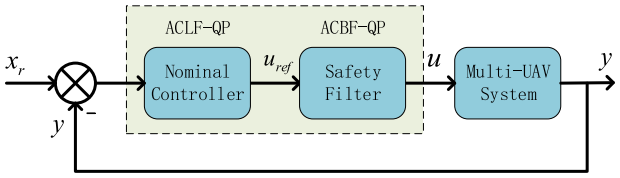

Fig. 2. Multi-UAV safe collaborative transportation control framework. The nominal controller u_{ref} is based on solving ACLF-QP to achieve trajectory tracking and the safety filter is based on solving ACBF-QP to realize obstacle avoidance.

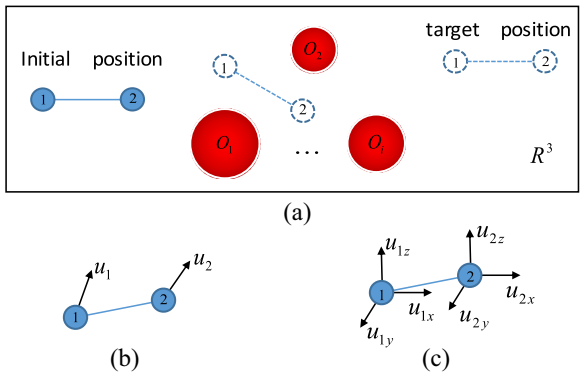

Fig. 3. (a) Schematic of dual UAVs working together to transport. (b) Composite object is controlled through the control inputs of the UAVs. (c) Control input components for dual UAVs in each direction.

spherical joints are used at the end points to ensure that the UAV dynamics are decoupled from the payload [32], [33].

Assumption 3: All obstacles explored in this article are spherical.

A. System Model

Consider an example of dual UAVs collaboratively transportation and avoiding obstacles in the three-dimensional workspace as shown in Fig. 3. There are i ($i > 1$) spherical obstacles O_i in this workspace and our control objective is to reach the target position from the initial position of the dual UAVs in collaborative transportation while avoiding obstacles.

As we all know, it is difficult to achieve accurate modeling of real control systems. Therefore, this article adopts a widely used double-integral dynamics with unknown parameter effects to represent the UAV dynamics, which is more accurate than the single-integral dynamics in [28]

$$\begin{aligned} \dot{x}_k &= v_k, \\ \dot{v}_k &= u_k - \frac{v_k}{m_k}\theta_k, \ k \in \{1, 2\} \end{aligned} \tag{24}$$

where x_k, v_k, u_k, and θ_k denote the real-time position, the velocity, the control input, and unknown constant parameter vector of the kth UAV, respectively. Also, $x_k = [x_{kx}, x_{ky}, x_{kz}]^{\mathrm{T}}$, $v_k = [v_{kx}, v_{ky}, v_{kz}]^{\mathrm{T}}$, and $u_k = [u_{kx}, u_{ky}, u_{kz}]^{\mathrm{T}}$ represent the components of real-time positions, velocities and control inputs in three dimensions, respectively. Moreover, $m_k \in \mathbb{R}^+$ is the known mass of the kth UAV and $\theta_k = [\theta_{k1}, \theta_{k2}, \theta_{k3}]^{\mathrm{T}}$.

B. Input Constraint

For actual UAV flight, the control input of the system is often limited to a certain range due to the physical constraints. For real system control analysis, the input constraint problem is often taken into account [34], [35]. The input constraint set U is represented as follows:

$$U = \left\{ u \in \mathbb{R}^6 : u_{\min} \le u \le u_{\max} \right\} \tag{25}$$

where $u = [u_1^{\mathrm{T}}, u_2^{\mathrm{T}}]^{\mathrm{T}}$, $u_{\min} = [u_{1\min}^{\mathrm{T}}, u_{2\min}^{\mathrm{T}}]^{\mathrm{T}}$, and $u_{\max} = [u_{1\max}^{\mathrm{T}}, u_{2\max}^{\mathrm{T}}]^{\mathrm{T}}$ denote the actual, lower and upper limits of the dual UAVs control inputs, respectively.

C. Rigid Body Constraint

In order to prevent the relative motion of the rigid payload between the UAVs, i.e., the rigid body from being compressed or stretched, this article considers the corresponding rigid body constraint.

Define the rigid body length at any time $t \ge 0$ as $\|x_{1,2}(t)\| = \|x_1(t) - x_2(t)\| = L$, where $x_1(t)$ and $x_2(t)$ are the real-time positions of two UAVs, respectively. The essence of the rigid body without deformation is that there is no velocity component in the direction of the rigid body, then, the rigid body constraint is expressed by the following vectorial inner product form:

$$\left\langle v_1(t) - v_2(t), x_{1,2}(t) \right\rangle = 0 \ \forall \ t \ge 0. \tag{26}$$

The constraint (26) can be rewritten as $F^{\mathrm{T}}u = 0$, where $F = [x_{1,2}^{\mathrm{T}}, -x_{1,2}^{\mathrm{T}}]^{\mathrm{T}}dt$, dt represents the sampling interval.

It is worth noting that there may be a deadlock situation for the system (24) due to the addition of (26). Deadlock indicates an unstable equilibrium, when this occurs, the unstable equilibrium can be broken by adding an arbitrarily small perturbation to bring it to the equilibrium point as described in [28].

Remark 4: By (26), the rigid body is not deformed by ensuring that the vector direction of the combined force is always vertical to the rigid body. However, since discrete sampling is still used in the actual data processing, a rigid body can only be considered nondeformed when the sampling interval is small enough.

D. Nominal Controller

By means of Definition 2, the nominal controller $u_{ref} = u_{\mathrm{ACLF}}$ can be obtained through the ACLF-QP framework as

$$u_{\mathrm{ACLF}} = \arg\min_{u \in \mathbb{R}^6} \ \frac{1}{2}u^{\mathrm{T}}Hu \tag{27}$$

$$\text{s.t.} \ \ L_f V(x) + L_Y V(x)\hat{\theta}_{j^*} + L_g V(x)u + \|L_Y V(x)\|\varphi \le -c_3 V(x) \tag{28}$$

$$u \in U \tag{29}$$

where H is a positive-definite matrix, φ is defined as in (11) and $\hat{\theta}_{j^*}$ is updated by (10) combining the logic switching mechanism.

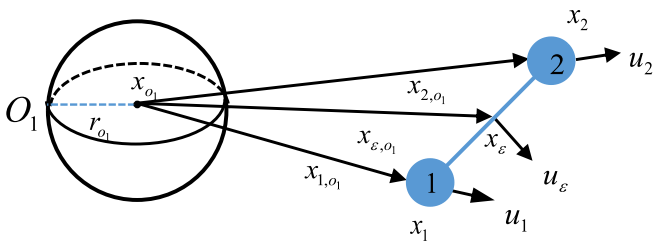

Fig. 4. Schematic of the composite object avoiding obstacle O_1.

E. Obstacle Avoidance

In what follows, consider the obstacle avoidance problem based on ACBF. The single obstacle case is first considered and the collision is avoided at any point on the composite object. Then, the theoretical results are extended to the case of collision avoidance with multiple obstacles.

1) Single Obstacle: Consider a single obstacle O_1 as shown in Fig. 4, where x_{o_1} and r_{o_1} denote the center position and radius of the spherical obstacle, respectively. The positions and inputs of the two UAVs are $\{x_1, x_2\}$ and $\{u_1, u_2\}$. The distance between the UAVs and the center of the obstacle are $x_{1,o_1} = x_1 - x_{o_1}$ and $x_{2,o_1} = x_2 - x_{o_1}$. A point on the composite object has position $x_\epsilon = \epsilon x_1 + (1-\epsilon)x_2$ for $\epsilon \in [0,1]$. Moreover, the effective control input for this point is $u_\epsilon = \epsilon u_1 + (1-\epsilon)u_2$. Further, the safety function can be defined by the distance expression $h(x_\epsilon) = \|x_{\epsilon,o_1}\| - r_{o_1}$, where $x_{\epsilon,o_1} = x_\epsilon - x_{o_1}$.

In order to reduce the number of constraints, the problem can be simplified to a single constraint problem of collision avoidance at the closest point of the composite object away from the obstacle. The closest point to the obstacle is obtained by the following optimization problem:

$$\epsilon_1^* = \arg\min_{\epsilon\in[0,1]} \|x_{\epsilon,o_1}\| - r_{o_1}. \tag{30}$$

Then, the safe set in the case of a single obstacle is defined as follows:

$$C_1 = \left\{x \in \mathbb{R}^3 : \|x_{\epsilon_1^*,o_1}\| - r_{o_1} \geq 0\right\} \tag{31a}$$

$$\partial C_1 = \left\{x \in \mathbb{R}^3 : \|x_{\epsilon_1^*,o_1}\| - r_{o_1} = 0\right\} \tag{31b}$$

$$\text{Int}(C_1) = \left\{x \in \mathbb{R}^3 : \|x_{\epsilon_1^*,o_1}\| - r_{o_1} > 0\right\}. \tag{31c}$$

Based on the analysis above, we propose the following candidate ACBF:

$$h_1\left(x_{\epsilon_1^*}\right) = \dot{h}\left(x_{\epsilon_1^*}\right) + \gamma h\left(x_{\epsilon_1^*}\right) \tag{32}$$

where γ is a positive constant. By Definition 3, one can get a safe constraint

$$L_f h_1\left(x_{\epsilon_1^*}\right) + L_Y h_1\left(x_{\epsilon_1^*}\right)\hat{\theta}_{j^*} + L_g h_1\left(x_{\epsilon_1^*}\right)u - \|L_Y h_1\left(x_{\epsilon_1^*}\right)\|\varphi \geq -\alpha\left(h_1\left(x_{\epsilon_1^*}\right)\right). \tag{33}$$

Theorem 3: The set C_1 is forward invariant for the system (24) if $h_1(x_{\epsilon_1^*})$ is an ACBF.

Proof: If $h_1(x_{\epsilon_1^*})$ is an ACBF, then $L_f h_1(x_{\epsilon_1^*}) + L_Y h_1(x_{\epsilon_1^*})\hat{\theta}_{j^*} + L_g h_1(x_{\epsilon_1^*})u - \|L_Y h_1(x_{\epsilon_1^*})\|\varphi \geq -\alpha(h_1(x_{\epsilon_1^*}))$. According to Theorem 2, one can obtain that $h_1(x_{\epsilon_1^*(t)}) \geq 0$ for any $t \in [0,\infty)$, i.e., $\dot{h}(x_{\epsilon_1^*(t)}) \geq -\gamma h(x_{\epsilon_1^*(t)})$. Since $x_{\epsilon_1^*(0)} \in C_1$ i.e., $h(x_{\epsilon_1^*(0)}) > 0$, one has $x_{\epsilon_1^*(t)} \in C_1$. Therefore, the set C_1 is forward invariant. ■

Remark 5: In summary, the collision avoidance problem for UAVs and payload composites is simplified to a single constraint associated with the point closest to the obstacle.

2) Multiple Obstacles: Now, consider the multiple obstacles case and define the closest points to the multiple obstacles O_l as $\epsilon_l^* = \arg\min_{\epsilon\in[0,1]} \|x_{\epsilon,o_l}\| - r_{o_l}$ by referring to the analysis in the previous section. Here, $x_{\epsilon,o_l} = x_\epsilon - x_{o_l}$, x_{o_l} and r_{o_l} denote the center position and radius of the lth spherical obstacle, where $l \in \{1,\ldots,i\}$. Then, define the following i safe sets and associated ACBFs for i obstacles:

$$C_l = \left\{x \in \mathbb{R}^3 : \|x_{\epsilon_l^*,o_l}\| - r_{o_l} \geq 0\right\} \tag{34a}$$

$$\partial C_l = \left\{x \in \mathbb{R}^3 : \|x_{\epsilon_l^*,o_l}\| - r_{o_l} = 0\right\} \tag{34b}$$

$$\text{Int}(C_l) = \left\{x \in \mathbb{R}^3 : \|x_{\epsilon_l^*,o_l}\| - r_{o_l} > 0\right\} \tag{34c}$$

and

$$h_l\left(x_{\epsilon_l^*}\right) = \dot{h}\left(x_{\epsilon_l^*}\right) + \gamma h\left(x_{\epsilon_l^*}\right),\ l = 1,\ldots,i \tag{35}$$

where $h(x_{\epsilon_l^*}) = \|x_{\epsilon_l^*,o_l}\| - r_{o_l}$, $x_{\epsilon_l^*,o_l} = x_{\epsilon_l^*} - x_{o_l}$ and the real safe set for the system (24) is $C = C_1 \cap C_2 \cap \ldots \cap C_i$. Further, the safe constraints for i obstacles can be obtained as follows:

$$L_f h_l\left(x_{\epsilon_l^*}\right) + L_Y h_l\left(x_{\epsilon_l^*}\right)\hat{\theta}_{j^*} + L_g h_l\left(x_{\epsilon_l^*}\right)u - \|L_Y h_l\left(x_{\epsilon_l^*}\right)\|\varphi \geq -\alpha\left(h_l\left(x_{\epsilon_l^*}\right)\right),\ \forall\, l \in \{1,\ldots,i\}. \tag{36}$$

F. Safety Filter

In order to meet the obstacle avoidance requirements, safety filter is introduced into the control framework of this article. Safety filter is used to adjust the control input by ACBF-QP, when there are obstacles in the environment, which ensures the safety of multi-UAV in collaborative transportation.

Specifically, we combine input (25), rigid body (26), and the safe constraints based on ACBFs (36) to define the following QP formulation:

$$u = \arg\min_{u\in\mathbb{R}^6} \ \frac{1}{2}(u - u_{ref})^{\mathrm{T}} H (u - u_{ref}) \tag{37}$$

$$\text{s.t.}\ \ F^{\mathrm{T}} u = 0, \tag{38}$$

$$u \in U, \tag{39}$$

$$L_f h_l\left(x_{\epsilon_l^*}\right) + L_Y h_l\left(x_{\epsilon_l^*}\right)\hat{\theta}_{j^*} + L_g h_l\left(x_{\epsilon_l^*}\right)u - \|L_Y h_l\left(x_{\epsilon_l^*}\right)\|\varphi \geq -\alpha\left(h_l\left(x_{\epsilon_l^*}\right)\right)$$
$$\forall\, l \in \{1,\ldots,i\} \tag{40}$$

where u_{ref} is the nominal controller and H is a positive-definite matrix. Also, φ is defined as in (11) and $\hat{\theta}_{j^*}$ is updated by (10) combining a logic switching mechanism.

Note that the safety filter used in this article is not a classical filter, it is defined to denote the adjustment of the nominal controller to ensure safety by ACBF-QP, which has been widely used in safety control [29], [36].

By solving the above QP problem, we can obtain the control input to avoid collision with obstacles during collaborative transportation of multi-UAV.

V. Simulation Results

In this section, in order to illustrate the effectiveness of the proposed method, simulation results of the UAV system (24) are presented by MATLAB.

We collaboratively transport a rigid payload of length $L = 1m$, mass $m = 1kg$ by two UAVs, and both UAVs are attached at the extremities of the payload via spherical joints. Also, the composite object controls the motion through the inputs of the two UAVs. The UAVs with dynamics (24) move in the $\mathbb{R}^3$ space, where acceleration is the control input of this system. Also, $m_1 = m_2 = 1kg$, $\theta_1 = \theta_2 = [1, 1, 1]^{\mathrm{T}}$, and the uncertain parameters belong to a compact set $S = [0, 2]^6$. The force provided for the payload by the kth UAV is $f_k = m_k u_k$, $k \in \{1, 2\}$. The real-time position of the payload is determined by the dual UAVs positions, and we can derive the following acceleration of the center of mass of the payload as [28]:

$$a_p = \frac{f_1 + f_2}{m} = \frac{m_1 u_1 + m_2 u_2}{m}. \tag{41}$$

There are six control inputs available $u = [u_{1x}, u_{1y}, u_{1z}, u_{2x}, u_{2y}, u_{2z}]^{\mathrm{T}}$. The initial positions of the UAVs are $x_1 = [-4, -5, -5]^{\mathrm{T}}$ m and $x_2 = [-3, -5, -5]^{\mathrm{T}}$ m. The target positions of the UAVs are $x_1 = [3, 4, 4]^{\mathrm{T}}$ m and $x_2 = [4, 4, 4]^{\mathrm{T}}$ m. The composite object needs to be moved from the initial positions to the target positions.

This simulation runs $N = 101$ identification models and sets initial estimates of parameters uniformly distributed in the compact set S. The filters are constructed as (3) and (4) with $A_0 = -I_{12}$, $\mu = 2$. The parameter update laws are given by (10) with $\rho = 0$. Choose the initial filter states as $\Omega(0) = 0$ and $\Omega_0(0) = [-4, -5, -5, 0, 0, 0, -3, -5, -5, 0, 0, 0]^{\mathrm{T}}$. The switching scheme is proposed as in Section III with $\alpha = \beta = 10$, $T_{\min} = 0.001$ s and $\xi = 0.005$.

This simulation considers four obstacles in their working environment. Choose the sphere center positions and radiuses as, O_1 : $x_{o_1} = [0, 0, 0]^{\mathrm{T}}$ m, $r_{o_1} = 1$m; O_2: $x_{o_2} = [-0.5, 1.5, 2.5]^{\mathrm{T}}$ m, $r_{o_2} = 1$ m; O_3 : $x_{o_3} = [-0.5, -2.5, -3]^{\mathrm{T}}$ m, $r_{o_3} = 1$ m; and O_4 : $x_{o_4} = [2.5, 2, 3]^{\mathrm{T}}$ m, $r_{o_4} = 1$ m. The upper bound and lower bound in input (25) are $u_{\max} = [20, 20, 20, 20, 20, 20]^{\mathrm{T}}$ m/s^2 and $u_{\min} = [-20, -20, -20, -20, -20, -20]^{\mathrm{T}}$ m/s^2. From the above input bound and dynamic (41), we are able to calculate the maximum acceleration of the payload as $a_{pmax} = u_{1\max} + u_{2\max}$ in this simulation. H is a identity matrix I_6 and $c_3 = 1$ in the QP problem (27). Moreover, the parameter $\gamma = 1$ in (35) and the class K function $\alpha_l(h_l) = 6h_l$ in (36). Also, choose $H = I_6$ in (37). The closest distances of the composite object to the four obstacles are d_{o1}, d_{o2}, d_{o3}, and d_{o4}. Distances of two UAVs to their respective target positions are d_{1r}, and d_{2r}. The simulation results are presented in Figs. 5–11. The sampling interval $dt = 0.01$ s in Figs. 5–10.

The trajectories of composite object and four obstacles in $\mathbb{R}^3$ space are displayed in Figs. 5 and 6. Fig. 5 shows the simulation trajectory without logic switching (the first model is selected at all times, i.e., the initial estimated parameters are chosen to be 0). Fig. 6 shows the trajectory with the logic switching mechanism. Figs. 5 and 6 show that the time for dual UAVs to safe collaborative transport is 20 and 18 s, respectively. Then, it can be clearly observed that the addition of the logic switching significantly reduces the collaborative transportation time (i.e., transient performance has

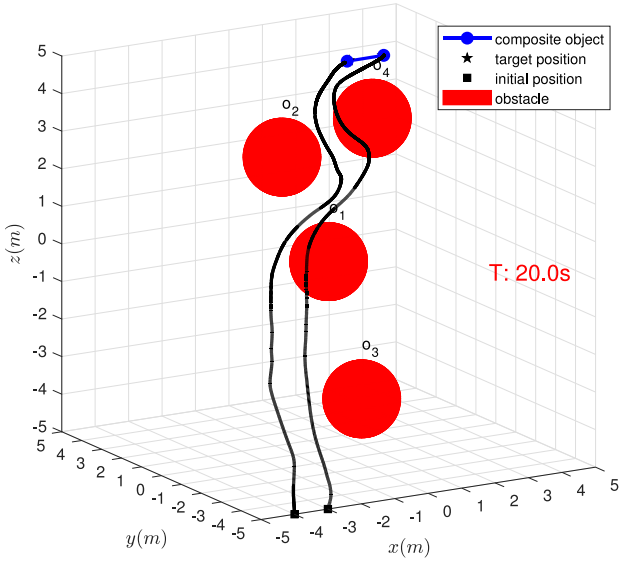

Fig. 5. Dual UAVs collaborative transport trajectory in $\mathbb{R}^3$ space with four obstacles via ACLF-QP combined with ACBF-QP in the absence of a logic switching mechanism.

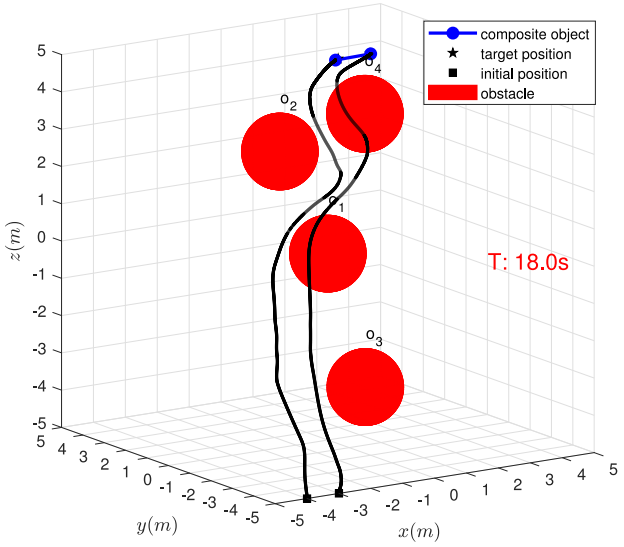

Fig. 6. Dual UAVs collaborative transport trajectory in $\mathbb{R}^3$ space with four obstacles via ACLF-QP combined with ACBF-QP in the presence of a logic switching mechanism.

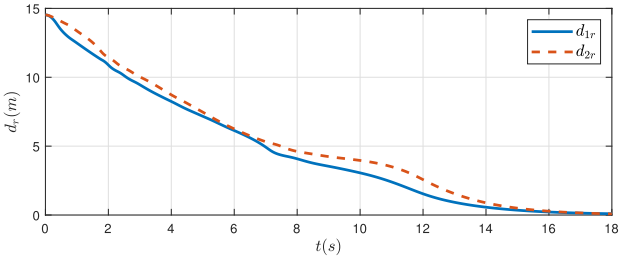

Fig. 7. Distances of two UAVs to their respective target positions via ACLF-QP combined with ACBF-QP.

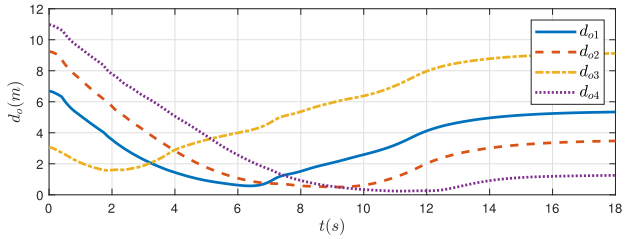

Fig. 8. Closest distances of the composite object to the four obstacles via ACLF-QP combined with ACBF-QP.

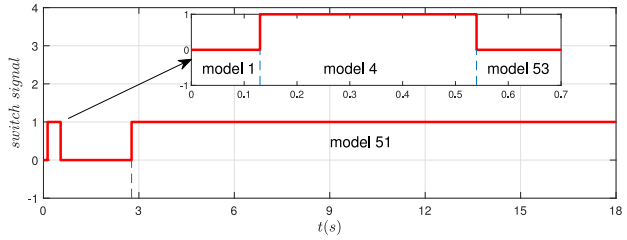

Fig. 9. Switching signal via multiple identification models combined with logic switching.

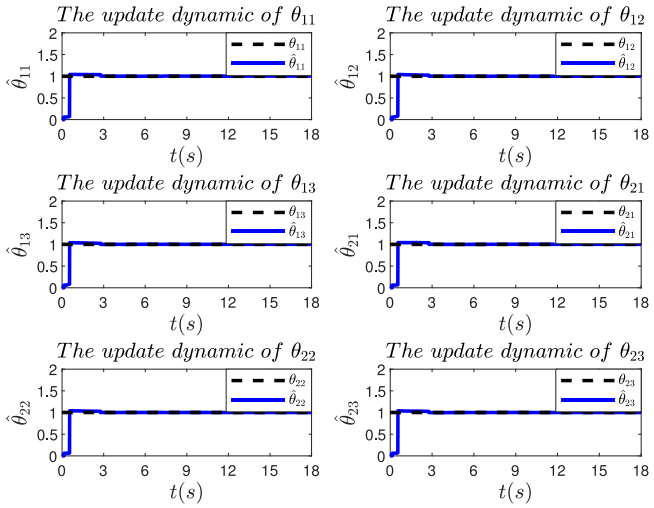

Fig. 10. Estimated parameter dynamics via multiple identification models combined with logic switching.

been improved). It is obvious that two UAVs reached their respective target positions over 18 s as reflected in Fig. 7. In addition, d_{o1}, d_{o2}, d_{o3}, and d_{o4} are obviously positive values at all times, i.e., the obstacle avoidance is achieved as shown in Fig. 8. The switching signal and real-time model are presented in Fig. 9. Also, a jump between 0 and 1 indicates that the current model is switched to another model. The ability of the update law to update uncertain parameters is illustrated in Fig. 10, where it can be seen that the estimated parameters converge approximately to their true values by ACLF-QP and ACBF-QP combined with a logic switching mechanism. Moreover, the rigid body has deformed even though the rigid body constraints are taken into account as described in Remark 4 by Fig. 11. For the deformation problem, it is obvious that the deformation value can be decreased by reducing the sampling interval as reflected in Fig. 11, where the sampling intervals dt are 0.01 and 0.001 s, respectively.

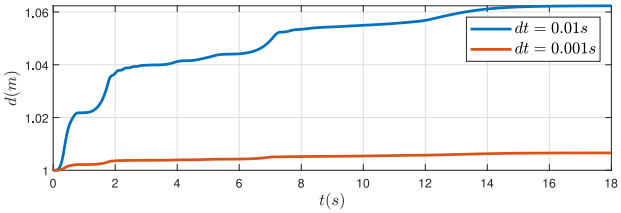

Fig. 11. Distance between two UAVs at different sampling intervals via ACLF-QP combined with ACBF-QP.

VI. Conclusion

In this article, the adaptive safe stabilization problem for a class of nonlinear control affine systems with parameter uncertainties has been studied. Two novel definitions of ACLF and ACBF have been presented, which used multiple identification models combined with a logic switching mechanism for parameter adaptation. Also, a multi-UAV safe collaborative transportation framework based on ACLF and ACBF has been presented to verify the effectiveness of the proposed design method.

In fact, there are many open problems that deserve further study. For example, when parameter uncertainties of nonlinear systems are not assumed to be constant, i.e., unknown time-varying parameters are considered, how to achieve adaptive safe stabilization and improve the transient performance of the system is a challenging problem.

References

[1] Y. Wu, L. Chen, L. Kong, J. Zhang, and M. Wang, "Research on application mode of large fixed-wing UAV system on overhead transmission line," in *Proc. IEEE Int. Conf. Unmanned Syst. (ICUS)*, 2017, pp. 88–91.

[2] A. Utsav, A. Abhishek, P. Suraj, and R. K. Badhai, "An IoT based UAV network for military applications," in *Proc. 6th Int. Conf. Wireless Commun., Signal Process. Netw. (WiSPNET)*, 2021, pp. 122–125.

[3] J. Tang, X. Li, J. Dai, and N. Bo, "Collision-free trajectory planning for multi-UAV coordinated ground attack mission under uncertainties," in *Proc. 11th Int. Conf. Intell. Human-Mach. Syst. Cybern. (IHMSC)*, 2019, pp. 89–92.

[4] J. Xiong and Y. Niu, "Guidance law for multi-UAVs collaborative ground target tracking under obstacle environment," in *Proc. 29th Chin. Control Decis. Conf. (CCDC)*, 2017, pp. 7219–7223.

[5] S. Zhuo and C. Li, "Source seeking of multi-UAV with obstacle avoidance," in *Proc. 37th Chin. Control Conf. (CCC)*, 2018, pp. 6955–6959.

[6] J. Cao, Y. Li, S. Zhao, and X. Bi, "Genetic-algorithm-based global path planning for AUV," in *Proc. 9th Int. Symp. Comput. Intell. Design (ISCID)*, 2016, pp. 79–82.

[7] J. Yu, H. Du, G. Wang, and L. Zhou, "Research about local path planning of moving robot based on improved artificial potential field," in *Proc. 25th Chin. Control Decis. Conf. (CCDC)*, 2013, pp. 2861–2865.

[8] A. D. Ames, X. Xu, J. W. Grizzle, and P. Tabuada, "Control barrier function based quadratic programs for safety critical systems," *IEEE Trans. Autom. Control*, vol. 62, no. 8, pp. 3861–3876, Aug. 2017.

[9] S. Hsu, X. Xu, and A. D. Ames, "Control barrier function based quadratic programs with application to bipedal robotic walking," in *Proc. Amer. Control Conf. (ACC)*, 2015, pp. 4542–4548.

[10] G. Wu and K. Sreenath, "Safety-critical control of a planar quadrotor," in *Proc. Amer. Control Conf. (ACC)*, 2016, pp. 2252–2258.

[11] L. Long and J. Wang, "Safety-critical dynamic event-triggered control of nonlinear systems," *Syst. Control Lett.*, vol. 162, Apr. 2022, Art. no. 105176. [Online]. Available: https://doi.org/10.1016/j.sysconle.2022.105176

[12] C. Huang and L. Long, "Safety-critical model reference adaptive control of switched nonlinear systems with unsafe subsystems: A state-dependent switching approach," *IEEE Trans. Cybern.*, early access, Apr. 25, 2022, doi: 10.1109/TCYB.2022.3164234.

[13] L. Long and Y. Hong, "Safety stabilization of switched systems with unstable subsystems," *Control Theory Technol.*, vol. 20, pp. 95–102, Feb. 2022, doi: 10.1007/s11768-022-00080-4.
[14] B. Yao, P. Lu, S. Yang, and X. Huang, "Trajectory tracking controller based on PID-NLADRC," in *Proc. Int. Conf. Comput. Netw., Electron. Autom. (ICCNEA)*, 2019, pp. 447–452.
[15] W. Ren and R. W. Beard, "CLF-based tracking control for UAV kinematic models with saturation constraints," in *Proc. 42nd IEEE Int. Conf. Decis. Control*, vol. 4, 2003, pp. 3924–3929.
[16] G. Ganga and M. M. Dharmana, "MPC controller for trajectory tracking control of quadcopter," in *Proc. Int. Conf. Circuit, Power Comput. Technol. (ICCPCT)*, 2017, pp. 1–6.
[17] S. Morales, J. Magallanes, C. Delgado, and R. Canahuire, "LQR trajectory tracking control of an omnidirectional wheeled mobile robot," in *Proc. IEEE 2nd Colombian Conf. Robot. Autom. (CCRA)*, 2018, pp. 1–5.
[18] L. Long and T. Hu, "Safety-critical control and optimization of nonlinear systems based on new forms of CLF-CBF-QP," *Control Theory Appl.*, vol. 39, no. 8, pp. 1387–1396, 2022.
[19] M. Krstić, I. Kanellakopoulos, and P. Kokotović, *Nonlinear and Adaptive Control Design*. New York, NY, USA: Wiley, 1995.
[20] L. Long, F. Wang, and Z. Chen, "Robust adaptive dynamic event-triggered control of switched nonlinear systems," *IEEE Trans. Autom. Control*, early access, Oct. 25, 2022, doi: 10.1109/TAC.2022.3217100.
[21] L. Long, Z. Wang, and J. Zhao, "Switched adaptive control of switched nonlinearly parameterized systems with unstable subsystems," *Automatica*, vol. 54, pp. 217–228, Apr. 2015.
[22] A. J. Taylor and A. D. Ames, "Adaptive safety with control barrier functions," in *Proc. Amer. Control Conf. (ACC)*, 2020, pp. 1399–1405.
[23] B. T. Lopez, J.-J. E. Slotine, and J. P. How, "Robust adaptive control barrier functions: An adaptive and data-driven approach to safety," *IEEE Control Syst. Lett.*, vol. 5, no. 3, pp. 1031–1036, Jul. 2021.
[24] A. Parikh, R. Kamalapurkar, and W. E. Dixon, "Integral concurrent learning: Adaptive control with parameter convergence using finite excitation," *Int. J. Adapt. Control Signal Process*, vol. 33, no. 12, pp. 1775–1787, 2019.
[25] A. Isaly, O. S. Patil, R. G. Sanfelice, and W. E. Dixon, "Adaptive safety with multiple barrier functions using integral concurrent learning," in *Proc. Amer. Control Conf. (ACC)*, 2021, pp. 3719–3724.
[26] D. D. Fan, J. Nguyen, R. Thakker, N. Alatur, A.-A. Agha-Mohammadi, and E. A. Theodorou, "Bayesian learning-based adaptive control for safety critical systems," in *Proc. IEEE Int. Conf. Robot. Autom. (ICRA)*, 2020, pp. 4093–4099.
[27] V. Dhiman, M. J. Khojasteh, M. Franceschetti, and N. Atanasov, "Control barriers in Bayesian learning of system dynamics," *IEEE Trans. Autom. Control*, vol. 68, no. 1, pp. 214–229, Jan. 2023.
[28] A. Hegde and D. Ghose, "Multi-UAV collaborative transportation of payloads with obstacle avoidance," *IEEE Control Syst. Lett.*, vol. 6, pp. 926–931, 2022.
[29] A. D. Ames, S. Coogan, M. Egerstedt, G. Notomista, K. Sreenath, and P. Tabuada, "Control barrier functions: Theory and applications," in *Proc. 18th Eur. Control Conf. (ECC)*, 2019, pp. 3420–3431.
[30] M. H. Cohen and C. Belta, "High order robust adaptive control barrier functions and exponentially stabilizing adaptive control Lyapunov functions," 2022, *arXiv:2203.01999*.
[31] X. Ye, "Nonlinear adaptive control using multiple identification models," in *Proc. 27th Chin. Control Conf.*, 2008, pp. 488–491.
[32] H. Nguyen, S. Park, and D. Lee, "Aerial tool operation system using quadrotors as rotating thrust generators," in *Proc. IEEE/RSJ Int. Conf. Intell. Robots Syst. (IROS)*, 2015, pp. 1285–1291.
[33] G. Li, D. Song, L. Sun, S. Xu, H. Wang, and J. Liu, "Static force-based modeling and parameter estimation for a deformable link composed of passive spherical joints with preload forces," *IEEE/CAA J. Automatica Sinica*, vol. 8, no. 11, pp. 1817–1826, Nov. 2021.
[34] F. Zhou, Y. Zhou, G. Jiang, and N. Cao, "Adaptive tracking control of quadrotor UAV system with input constraints," in *Proc. Chin. Control Decis. Conf. (CCDC)*, 2018, pp. 5774–5779.
[35] P. Panyakeow and M. Mesbahi, "Deconfliction algorithms for a pair of constant speed unmanned aerial vehicles," *IEEE Trans. Aerosp. Electron. Syst.*, vol. 50, no. 1, pp. 456–476, Jan. 2014.
[36] V. Freire and X. Xu, "Flatness-based quadcopter trajectory planning and tracking with continuous-time safety guarantees," *IEEE Trans. Control Syst. Technol.*, early access, Mar. 13, 2023, doi: 10.1109/TCST.2023.3250954.